Structural mechanics of the mosquito heart and its function in bidirectional hemolymph transport

Justin D. Glenn*, Jonas G. King* and Julián F. Hillyer[†]

Department of Biological Sciences and Institute for Global Health, Vanderbilt University, VU Station B 35-1634, Nashville, TN 37235-1634, USA

*These authors contributed equally to this work
[†]Author for correspondence (julian.hillyer@vanderbilt.edu)

SUMMARY

The insect circulatory system transports nutrients, signaling molecules, wastes and immune factors to all areas of the body. The primary organ driving circulation is the dorsal vessel, which consists of an abdominal heart and a thoracic aorta. Here, we present qualitative and quantitative data characterizing the heart of the mosquito, *Anopheles gambiae*. Visual observation showed that the heart of resting mosquitoes contracts at a rate of 1.37 Hz (82 beats per minute) and switches contraction direction, with 72% of contractions occurring in the anterograde direction (toward the head) and 28% of contractions occurring in the retrograde direction (toward the tip of the abdomen). The heart is tethered to the midline of the abdominal tergum by six complete and three incomplete pairs of alary muscles, and propels hemolymph at an average velocity of 8 mm s^{-1} by sequentially contracting muscle fibers oriented in a helical twist with respect to the lumen of the vessel. Hemolymph enters the heart through six pairs of incurrent abdominal ostia and one pair of ostia located at the thoraco-abdominal junction that receive hemolymph from the abdominal hemocoel and thoracic venous channels, respectively. The vessel expels hemolymph through distal excurrent openings located at the anterior end of the aorta and the posterior end of the heart. In conclusion, this study presents a comprehensive revision and expansion of our knowledge of the mosquito heart and for the first time quantifies hemolymph flow in an insect while observing dorsal vessel contractions.

Supplementary material available online at http://jeb.biologists.org/cgi/content/full/213/4/541/DC1

Key words: *Anopheles gambiae*, mosquito, contraction, heart, heartbeat, hemolymph.

INTRODUCTION

Insects have an open circulatory system for the transport of nutrients, wastes and signaling molecules (Klowden, 2007; Nation, 2008). In addition, the insect circulatory system functions in thermoregulation, promoting ventilation through the tracheal system, and the circulation of humoral immune molecules and immune blood cells (hemocytes) that survey tissues for foreign invaders. The general anatomy of the insect circulatory system consists of a dorsal vessel that extends the length of the insect, an open body cavity (hemocoel), and numerous accessory pulsatile organs (Klowden, 2007; Nation, 2008). The dorsal vessel is a tube that is divided into a thoracic aorta and an abdominal heart that contains valves called ostia, which allow hemolymph to enter the lumen. Hemolymph inside the dorsal vessel is pumped toward the head or the tip of the abdomen where it empties into the hemocoel and moves until it reenters the heart. Because of the passive nature of hemolymph flow in the hemocoel, insects also use a series of autonomous accessory pulsatile organs to pump hemolymph to the appendages and other regions that would otherwise experience low flow rates (Pass, 2000). However, insects have evolved over 400 million years so it is not surprising that there are numerous variations to this general plan, especially given the broad range of insect sizes and behaviors. Variations include the presence or absence of segmental blood vessels originating from the heart (Hertel and Pass, 2002), various forms of ostia (Pass et al., 2006), a closed *versus* open posterior heart (Chapman, 1998; Nation, 2008), differing populations of circulating hemocytes (Hillyer and Christensen, 2002), and differing ratios of forward to backward hemolymph flow (Jones, 1977). Based on recent

observations in *Drosophila* and other insects (Lee and Socha, 2009; Sláma, 2003; Wasserthal, 2007), it has become clear that the circulatory system of insects is far more complex than originally thought.

Within the order Diptera, considerable research efforts have been aimed at characterizing the structure and development of the *Drosophila* (suborder: Brachycera) heart (Tao and Schulz, 2007; Wasserthal, 2007). However, the hearts of dipterans from the suborder Nematocera have been largely ignored, a surprising fact given the ecological and public health significance of an insect group that includes the mosquitoes, sand flies, black flies and biting midges. Among these, mosquitoes (Culicidae) are the most epidemiologically significant pests and disease vectors, as they transmit deadly human and animal pathogens such as the causative agents of malaria, lymphatic filariasis and dengue hemorrhagic fever. During their natural life cycle, these pathogens are ingested with infective blood meals, cross the midgut epithelium, and enter the hemocoel, where they migrate to the salivary glands or mouthparts (Hillyer et al., 2007; Matuschewski, 2006; Salazar et al., 2007). Understanding the physiological basis of hemolymph flow may increase our knowledge on how these parasites undergo this obligate migration.

Most of what is known about the anatomy of the mosquito circulatory system comes from experiments performed over 20 years ago (Clements, 1992b), with the majority of the data originating from two publications that analyzed the circulatory systems of *Anopheles quadrimaculatus* and *Anopheles maculipennis* (Iaguzhinskaja, 1954; Jones, 1954). The anatomical descriptions in those studies are very

informative but were limited by the methodologies available at the time, and include observations that are in conflict with one another or have since been proved incorrect. For example, there are conflicting reports regarding the number of alary muscle pairs present in the mosquito abdomen (Jones, 1977), and, contrary to what was previously reported (Jones, 1977), several subsequent studies have identified and characterized circulating hemocytes in mosquitoes of the genus *Aedes* (Castillo et al., 2006; Hillyer and Christensen, 2002). Here, we employ a novel approach to the study of the insect dorsal vessel and present qualitative and quantitative data characterizing the structural mechanics of the mosquito heart.

MATERIALS AND METHODS
Mosquito rearing and maintenance

Mosquitoes were reared and maintained in an environmental chamber at 27°C, 75% relative humidity, with a 12h:12h light:dark photoperiod and a 30min crepuscular period at the beginning and end of each light cycle. *Anopheles gambiae* Giles *sensu stricto* (SUA2La hybrid) larva were hatched in distilled water, transferred to plastic pans, and fed a slurry of ground koi fish food and baker's yeast. Following pupation, mosquitoes were transferred to 4.73l containers with a fine-mesh marquisette top. Upon emergence, 10% sucrose-soaked pads were placed on top of the marquisette and adults allowed to feed *ad libitum*. All experiments were performed on adult female mosquitoes at 5days post emergence.

Observation of live mosquito hearts

Mosquitoes were anesthetized on ice for less than 1min and restrained dorsal-side-up on Sylgard 184 silicone plates (Dow Corning Corp, Midland, MI, USA) or agarose slides by placing 0.15mm diameter pins gently against (not through) the anterior pronotal lobe (Fig. 1A). The wings were then teased laterally and an additional pin inserted through a non-vascular area (e.g. cell R3) of each wing without creating horizontal or vertical tension. This non-invasive restraint method prevented live mosquitoes from attempting to fly while maintaining them in a natural position that allowed for visual observation of the beating heart.

The heart of mosquitoes maintained at approximately 24°C was imaged through the dorsal cuticle using bright-field illumination on a Nikon 90i light microscope (Nikon Corp., Tokyo, Japan) connected to a Photometrics CoolSNAP HQ2 high sensitivity monochrome CCD camera (Roper Scientific, Ottobrunn, Germany). Digital videos of 1-min duration were acquired for each mosquito at 30 frames per second using Nikon Advanced Research NIS-Elements software. Initially, contractions were compared to the flow of endogenous particles or intrathoracically injected 2μm diameter red fluorescent (580/605 nm) carboxylate-modified latex microspheres (Invitrogen, Carlsbad, CA, USA; see below) to determine the relationship between contraction mechanics and pulse direction. Then, quantitative analyses were carried out by manually annotating contractions and contraction directionality over the entire 60-s recordings of unmanipulated mosquitoes (mosquitoes that had not been injected or otherwise manipulated except for restraint on Sylgard or agarose plates). Three cohorts of 10 mosquitoes each were analyzed. Each cohort was reared independently and originated from different egg batches. Contraction rate (frequency) is presented as hertz (Hz; contractions s^{-1}).

Particle tracking and measurement of hemolymph flow velocity

Individual mosquitoes were restrained on Sylgard plates as described above and a finely pulled glass capillary needle was inserted through the anepisternal cleft, also defined as the membrane located between the paratergite, the postspiracular area and the mesepisternum in the lateral mesothorax. A volume of 40–50 nl of 0.1 mol l^{-1} phosphate-buffered saline (PBS; pH 7.0) containing a 1:10,000 dilution of 2 μm diameter red fluorescent microspheres was injected into the hemocoel of live mosquitoes and allowed to mix with the hemolymph. Once in circulation, videos of 1-min duration were acquired by low-level fluorescence imaging through the dorsal cuticle using a Nikon SMZ1500 stereomicroscope connected to a Photometrics CoolSNAP HQ2 camera. Videos were captured using either fixed frame rates (24, 14 and 10 frames s^{-1} for supplementary material Movies 2, 5 and 7, respectively) or the 1-frame acquisition mode in NIS-Elements (an average rate of 27 and 48 frames s^{-1} for supplementary material Movies 4 and 6, respectively). The manual feature of the NIS-Elements' Object Tracking module was then used to track individual particles or groups of particles as they entered and moved through the mosquito heart. Distance traveled and velocity were calculated both from frame-to-frame and for the entire path tracked. For hemolymph velocity analyses, 100 particles in 10 mosquitoes were independently tracked in each contraction direction and only particles that could be tracked for a distance greater than 500 μm were used in the analyses.

Light and fluorescence microscopy of aldehyde-fixed mosquito whole mounts

For fluorescence labeling of muscle, live mosquitoes were intrathoracically injected with 0.25 μl of a solution consisting of 1% Triton X-100 (Thermo Fisher Scientific Inc., Waltham, MA, USA), 0.3 μmol l^{-1} phalloidin–Alexa Fluor 488 (Invitrogen), and 8% formaldehyde (Electron Microscopy Sciences, Hatfield, PA, USA) in PBS and allowed to incubate for 15 min. For mosquitoes to be viewed as undissected whole mounts, a small cut was made in the eighth abdominal segment and specimens were rinsed by intrathoracically injecting PBS and allowing the buffer to exit through the tip of the abdomen. Whole abdomens were then visualized from the exterior on glass depression slides. For mosquitoes to be viewed as dissected whole mounts, abdomens were dissected along a coronal plane to obtain the dorsal halves, washed three times for 5 min each with 0.1% Tween 20 in PBS, and mounted on glass slides using Aqua-Poly/Mount (Polysciences Inc., Warrington, PA, USA). To counterstain the ostia, some specimens were injected with a 1:20 dilution of India ink in PBS several hours prior to injection of phalloidin–Alexa Fluor 488. Samples were imaged under bright-field and fluorescence illumination using a Nikon 90i microscope connected to a Photometrics CoolSNAP HQ2 camera.

For three-dimensional rendering, Z-stacks were created by using a linear encoded Z-motor to acquire images at 0.7 μm Z-intervals for a total Z-range of 40 μm. Z-stacks were then quantitatively deconvolved using the AQ 3D Blind Deconvolution module of NIS Elements and rendered using the volume view feature. For the rendering of detailed fluorescence images with extended focal depth, Z-stacks of whole mounts were acquired and all images in a stack combined to form a focused image using the Extended Depth of Focus (EDF) module of NIS Elements.

Embedding, sectioning, and visualization of aldehyde-fixed mosquito abdomens

Mosquitoes were severed in the first and eighth abdominal segments. The abdomens were dissected along a coronal plane to obtain the dorsal halves, fixed for approximately 12 h in 4% formaldehyde in 0.1 mol l^{-1} phosphate buffer (pH 7.0), and dehydrated through a

graded ethanol series. Specimens were then infiltrated with JB4-Plus resin (Electron Microscopy Sciences), and embedded in polyethylene molding trays anaerobically sealed with block holders and wax. Sections were cut (2.5 μm thick) with a glass knife on a Sorvall JB-4 microtome (Sorvall, Newtown, CT, USA) and placed on glass slides. Sections were stained for 15 min with Gill's Hematoxylin, rinsed with water, stained for 5 min with Eosin Y, and rinsed again with water. Slides were then dried, mounted with Poly-Mount (Polysciences Inc.), and imaged using differential interference contrast (DIC) optics on a Nikon 90i microscope connected to a Nikon DS-Fi1 high-definition color CCD camera.

RESULTS

The mosquito heart pumps hemolymph in both anterograde and retrograde directions

Light and fluorescence microscopy through the cuticle of gently immobilized live mosquitoes confirmed that the dorsal vessel is the primary hemolymph-pumping organ in mosquitoes (Fig. 1A; supplementary material Movie 1). It extends from the posterior of the abdomen to the head and is divided into two anatomically and functionally distinct regions: the heart and the aorta. The heart is an unbranched tube that runs immediately underneath the dorsal midline of the abdominal tergum and is the focus of this study. The aorta is located in the thorax and serves as a conduit for hemolymph actively propelled by the heart (Klowden, 2007; Nation, 2008).

Because of heavy sclerotization in the dorsal portion of the thorax, the aorta of live mosquitoes was not definitively identified in this study.

Analysis of the contraction dynamics of the heart, along with the concurrent visualization of the flow of endogenous lipid droplets and air bubbles, demonstrated that the heart is a dynamic organ which alternates between pumping hemolymph in anterograde (toward the head) and retrograde (toward the tip of the abdomen) directions. Quantitative assessment of contraction mechanics showed that the dorsal vessels of unmanipulated 5-day-old mosquitoes in their resting state contracted at a rate of 1.37±0.15 Hz (± s.d.; 82.4 beats per minute; Fig. 1B). Interestingly, the direction in which the heart contracts reversed 5.3±1.78 times per minute, but the contraction rate did not change with contraction direction (t-test P=0.8398): anterograde contractions occurred at a rate of 1.38±0.12 Hz and retrograde contractions at a rate of 1.35±0.23 Hz. Although the frequency of heart contractions was the same regardless of pulse direction, the heart spent more time, and hence contracted more, in the anterograde direction (t-test P<0.0001). The average number of anterograde contractions in a 60 s recording was 59.1±2.46 (±s.d.) whereas the average number of retrograde contractions in a 60 s recording was 23.3±8.23 (Fig. 1C). Hence, 71.7±5.5% of contractions were in the anterograde direction, depositing hemolymph in the head, whereas 28.3±5.5% of the contractions occurred in the retrograde direction, depositing
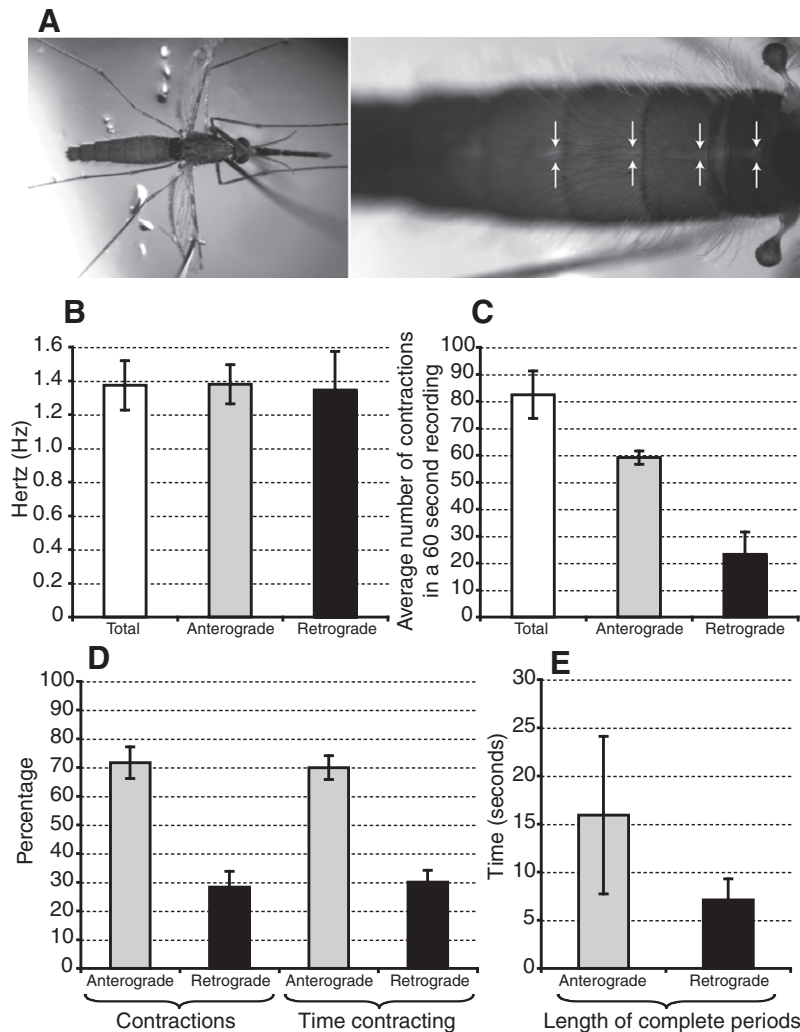

Fig. 1. Quantitative analyses of heart contractions. (A) Mosquito restraint system showing pins placed against the anterior pronotal lobe and through non-vascular areas of the wings. Note that no pins are inserted through the body cuticle and the dorsal vessel and dorsal diaphragm are clearly visible under incandescent light (arrows). (B) The mosquito heart rate. Peristaltic contractions can reverse direction, but the contraction rate does not change with contraction direction. Mean total rate was 1.37 Hz. (C) Contractions in the anterograde and retrograde direction. In 60 s recordings, the hearts contracted on average 59 times in the anterograde direction and 23 times in the retrograde direction. (D) Percentage of contractions in each direction. Approximately 72% of the contractions occurred in the anterograde direction and 28% in the retrograde direction. In parallel, the time spent contracting in each direction was similar. (E) Duration of anterograde and retrograde flow. The heart of resting mosquitoes switches contraction direction an average of 5.3 times per minute, contracting for 16 consecutive seconds in the anterograde direction before switching and contracting for 8 consecutive seconds in the retrograde direction. (N=3 independent cohorts of 10 mosquitoes each.)

hemolymph in the last segment of the abdomen (Fig. 1D). From these data it is apparent that the mosquitoes spent 70.0±4.12% of the time contracting the heart toward the head and 30.0±4.12% of the time contracting the heart toward the tip of the abdomen, suggesting that hemolymph flow is primarily directed toward the head (Fig. 1D). When we analyzed data from complete periods, the length of each period was highly variable: anterograde periods averaged 15.9±7.1 s whereas retrograde periods averaged 8.2±2.2 s (Fig. 1E). Finally, these observations were confirmed by visualizing the trajectory of intrathoracically injected red fluorescent microspheres in a parallel group of mosquitoes.

Peristaltic contractions of the heart drive hemolymph flow but the contraction mechanism changes with propulsion direction

Detailed high magnification observation of the portion of the heart located in the second abdominal segment as well as the entire abdomen of unmanipulated mosquitoes revealed that, regardless of directionality, hemolymph propulsion is accomplished by wave-like peristaltic contractions that are equivalent to the transition of systolic (contraction) and diastolic (relaxation) phases in each abdominal segment (supplementary material Movies 1, 2). The direction of the wave-like sequential contractions of the heart dictates the direction of hemolymph flow. That is, peristaltic contractions originating in the posterior of the heart travel toward the head and propel hemolymph in the anterograde direction. Conversely, peristaltic contractions that begin near the junction between the thorax and the abdomen and progress toward the tip of the abdomen propel hemolymph in the retrograde direction. Although peristalsis drives both anterograde and retrograde contractions, the contraction mechanism changes with propulsion direction. Anterograde contractions involve a smooth peristalsis where systole does not completely close the dorsal vessel. By contrast, retrograde contractions seem more forceful and the systole phase appears to involve a complete constriction of the heart.

Hemolymph flows through the heart at velocities greater than 8 mm s^{-1}

Tracking of intrathoracically injected red fluorescent microspheres showed that flow through the dorsal vessel is rapid and parallels the high rate of heart contractions. Also, similar to the data on contraction rate, no significant difference was seen between anterograde and retrograde hemolymph velocity (*t*-test *P*=0.391; Fig. 2; supplementary material Movie 2). On average, hemolymph flowed in the anterograde direction at a velocity of 8.03±2.17 mm s^{-1} (± s.d.) and in the retrograde direction at a velocity of 8.29±2.01 mm s^{-1}. All microspheres were tracked for a minimum distance of 0.5 mm and the average distances tracked were 1.28±0.32 mm (± s.d.) in the anterograde direction and 1.43±0.30 mm in the retrograde direction. The maximum and minimum average velocities for the entire paths tracked were also similar between groups: the anterograde maximum was 14.75 mm s^{-1} and the retrograde maximum was 13.47 mm s^{-1} whereas the anterograde minimum was 4.11 mm s^{-1} and the retrograde minimum was 3.73 mm s^{-1}. Across shorter distances hemolymph can move even faster, with frame-to-frame maximum velocities of 19.62 mm s^{-1} and 22.38 mm s^{-1} for anterograde and retrograde directions, respectively.

Overall, the bolus-like travel of microspheres through the dorsal vessel confirmed the morphological observations showing that in both directions a peristaltic pump drives hemolymph propulsion. Because the diameters of the dorsal vessel (which can exceed 50 μm) and circulating hemocytes are considerably greater than the diameter of the microspheres tracked (2 μm), we believe that the velocity of
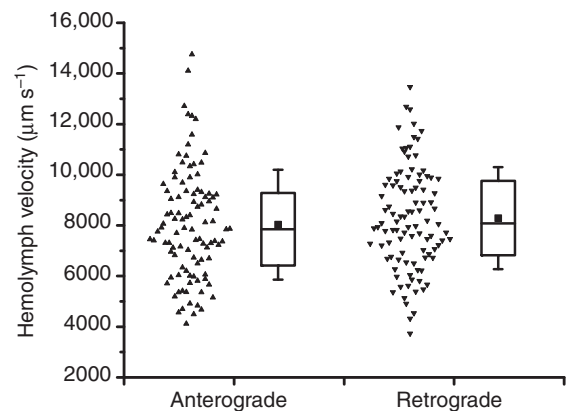

Fig. 2. Velocity of hemolymph flow through the heart. Tracking of injected red fluorescent microspheres showed that hemolymph travels in anterograde and retrograde directions at an average speed greater than 8 mm s^{-1}. For each flow direction (anterograde and retrograde), raw data are plotted on the left and a summary of the data showing the mean (solid square), median (center line), 50% of the data (box), and standard deviation (bars) is plotted on the right.

particles is an accurate representation of the velocity of hemolymph flow. Furthermore, similar results were obtained when soluble Alexa Fluor dye was injected instead of beads.

Hemolymph flow is accomplished by the sequential contraction of muscle fibers arranged in a helical twist with respect to the lumen of the heart

Light microscopic visualization of live mosquitoes, sectioned mosquitoes, and mosquitoes that were formaldehyde-fixed and the musculature stained with Alexa-Fluor-488-conjugated phalloidin showed that the heart is a muscular tube that spans the length of the abdomen (Fig. 3). When viewed from posterior to anterior, cardiac striated muscle fibers were seen to form a clockwise helical twist with respect to the lumen of the heart, and it is the directional sequential contraction of these fibers that propels hemolymph from one end of the organism to the other.

Heart contractions are aided by the support of six complete pairs of bilaterally symmetrical alary muscles that span all abdominal sutures with the exception of the junction between the seventh and eight abdominal segments (posterior suture), where musculature resembling the anterior end of two alary muscle pairs attach the posterior end of the heart to the tergum (Fig. 3A,C–E). Alary muscles originate in the lateral edge of the tergum (near the junction between the tergites and the pleurites) in the anterior portion of each abdominal segment and initially fan out into two large bundles, each of which promptly subdivides into two bundles, and each divides again into between 10 and greater than 30 myofibers that bind the heart, forming baskets that tether the dorsal vessel to the abdominal cuticle. The end point of alary muscle fibers varies with their location, but they firmly bind the dorsal vessel, with most fibers attaching to the ventral half of the heart (Fig. 3A,E; supplementary material Movie 3). Fibers at the center of the basket bind the heart at a 90 deg. angle before binding myofibers that originate from the paired alary muscle on the opposite side of the heart (Fig. 3A). Fibers at the anterior and posterior edges of the basket bind the heart at a sharp angle and continue on to bind myofibers from alary muscles that originate in adjoining abdominal segments (Fig. 3A). The tension created by the binding of alary muscles to the heart causes an expansion of the cross-sectional area of the heart, giving the heart
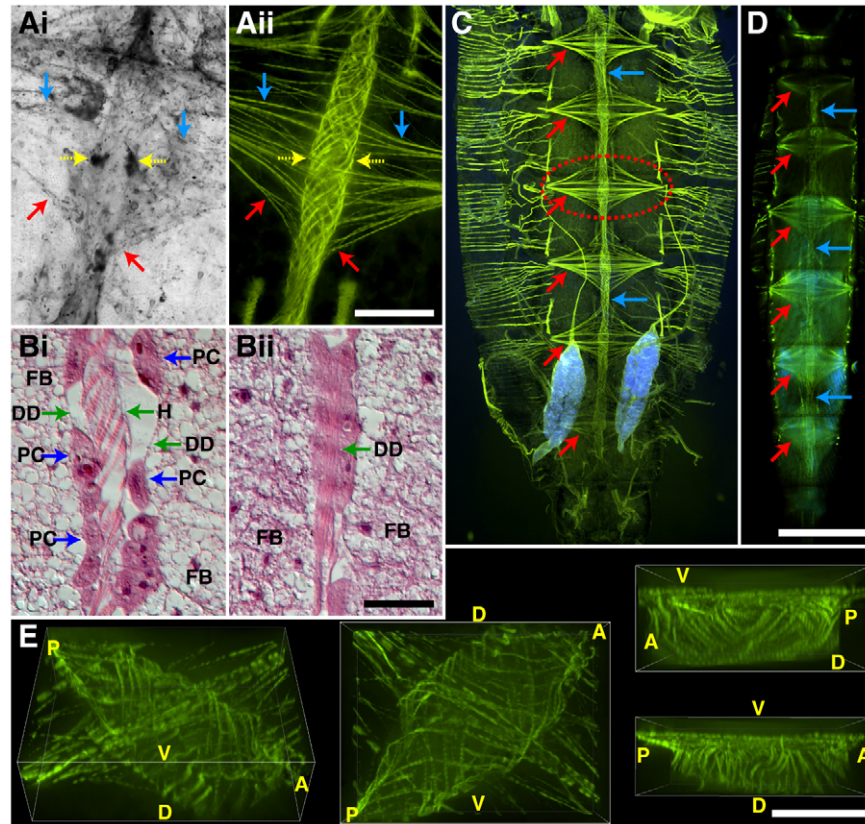
Fig. 3. Musculature associated with the mosquito heart. All images are oriented with anterior towards the top (with the exception of E), and Aii, C, D and E show muscles fluorescently labeled with phalloidin–Alexa Fluor 488 (green). (A) Bright-field (Ai) and fluorescence (Aii) images of dissected whole mounts showing that muscle fibers are arranged in a clockwise helical twist that extends toward the thorax. Alary muscle fibers bind the heart and either join myofibers that originate from the opposite alary muscle (blue arrows) or join alary muscle fibers that originate in neighboring abdominal segments (red arrows). Paired ostia are labeled with India ink (yellow dotted arrows). (B) Histological sections of mosquito abdomens in two different coronal planes (i and ii) showing the clockwise helical spiraling of cardiac musculature (heart; H), the dorsal diaphragm (DD), pericardial cells (PC) and fat body (FB). (C) Fluorescence image of dissected whole mount showing that the mosquito heart spans the length of the abdomen and contains helically oriented musculature (blue arrows). Six complete pairs of alary muscles span the abdominal sutures (red arrows; one complete pair inside dotted circle) except the suture between the last two abdominal segments. Ovaries are stained blue with Hoechst 33342. (D) Fluorescence image through the cuticle of a fixed mosquito showing that the dorsal vessel is located immediately underneath the dorsal cuticle (e.g. blue arrows) and showing the six complete pairs of alary muscles (red arrows). (E) Three-dimensional rendering of a segment of the mosquito heart, showing the clockwise helical spiraling of muscle fibers and the alary muscles associated with it. A, anterior; P, posterior; D, dorsal; V, ventral. Scale bars, (A) 75 μm; (B) 40 μm; (C,D) 500 μm; (E) 20 μm.

a segmented appearance that resembles six chambers joined by tapered segments. In addition to supporting the mosquito heart, alary muscles, along with connective tissue, form an incomplete dorsal diaphragm that delineates the pericardial sinus containing the heart and pericardial cells, and separates them from the perivisceral sinus (Fig. 3B). It is possible that this dorsal diaphragm may create a filter that limits the size of particles entering the heart.

Hemolymph enters the heart through incurrent ostia and thoracic venous channels, and exits through excurrent distal openings

Tracking of red fluorescent microspheres in hundreds of videos showed that hemolymph enters the heart through 14 abdominal and thoraco-abdominal ostia (Fig. 4; supplementary material Movie 4). During anterograde flow, particles unidirectionally entered the lumen of the heart through ostia whereas during retrograde flow particles neither entered nor exited, suggesting that abdominal ostia open during the diastole phase of each anterograde contraction while remaining completely closed when the heart is contracting in the retrograde direction (Fig. 4). As particles entered the heart through the ostia, their velocity changed from as slow as a virtual standstill

while in the hemocoel to speeds in excess of 4 mm s^{-1} in the lumen of the heart (Fig. 4B).

Twelve abdominal ostia were seen to be located as pairs on the lateral wall of the heart near the anterior portion of segments 2, 3, 4, 5, 6, and 7. Each ostium is composed of two muscular funnel-shaped lips that protrude into the lumen of the heart at an anterior angle (Fig. 5), and are morphologically similar to the one-way incurrent ostia described in other insects (no excurrent ostia were structurally or functionally observed in *Anopheles* mosquitoes) (Pass et al., 2006). The location of the ostia is dorsal of the lateral midline of alary muscles but slightly posterior, and these valves are within the pericardial sinus delineated by the incomplete dorsal diaphragm formed by the alary muscles and accompanying connective tissue (Fig. 3A). Visual observation of the alary muscles did not conclusively show that they directly bind each ostium or directly participate in the peristaltic contraction of the vessel. However, because the ostia are located near the center of each alary basket and complete alary muscles are only present in regions surrounding the ostia (complete pairs are not present in the suture between segments 7 and 8 where there are no ostia; see below), it is possible that the alary muscles may indirectly control the opening and closing
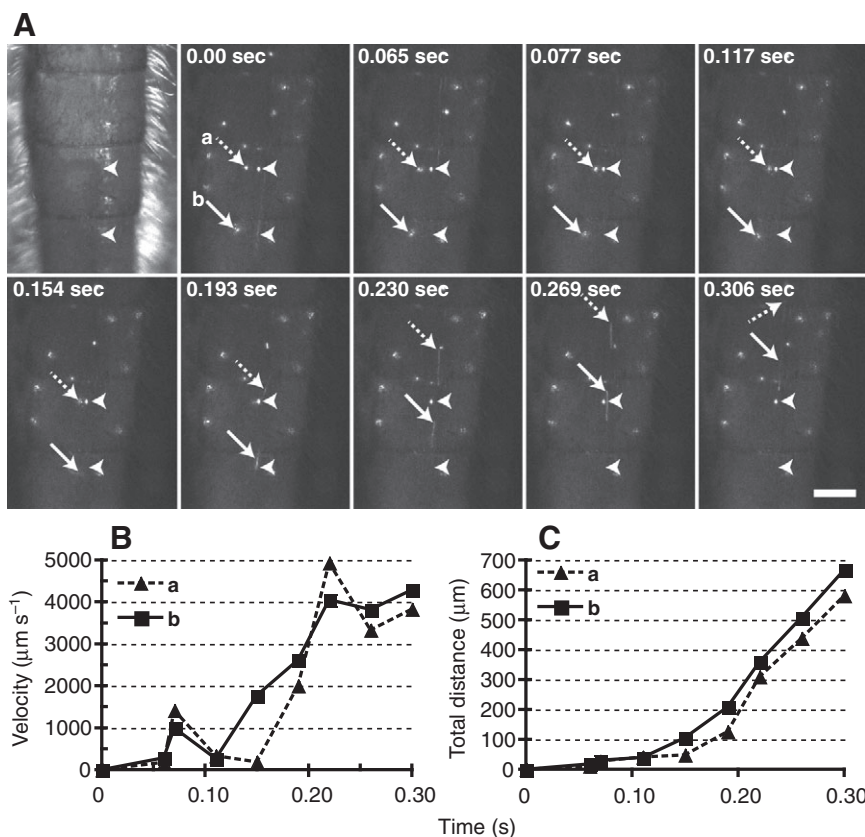
Fig. 4. Tracking of particles as they enter the heart through ostia and travel in the anterograde direction. (A) Bright-field (top left) and sequence of consecutive fluorescence images tracking two 2 μm diameter red fluorescent microspheres as they enter through ostia (microsphere a, dotted arrow; microsphere b, arrow; ostia, arrowhead). Both particles enter the lumen of the heart at the 0.193 s mark. Scale bar, 200 μm. (B) Velocity plot showing that in the hemocoel particles move slowly but once inside the heart they travel at speeds in excess of 4 mm s^{-1}. (C) Distance plot showing that during the 0.193 s the particles were tracked in the hemocoel they traveled less than 100 μm whereas during the 0.113 s they were tracked inside the heart they traveled more than 500 μm.

of the ostia and pull the heart into diastolic position when the cardiac helical muscles are relaxed. This is not in conflict with the opening of ostia only during anterograde flow as the angular nature of the ostial lips may prevent them from opening when hemolymph is flowing in the retrograde direction.

The heart is attached to the aorta at the thoraco-abdominal junction by musculature resembling the posterior portion of a pair of alary muscles (Fig. 6). As mentioned, during retrograde flow hemolymph does not enter the heart through abdominal ostia. Instead, hemolymph flowing through venous channels in the lateral-posterior thorax enters the heart through what appears to be a single pair of ostia located in the anterior end of the heart at the thoraco-abdominal junction (Fig. 6A,B; supplementary material Movies 5 and 6). Following entry into the vessel, hemolymph flow is dictated by the direction of the peristaltic contractions of the heart. Mosquito venous channels appear to be homologous to those recently discovered in *Drosophila* (Wasserthal, 2007), and all hemolymph propelled in the retrograde direction appears to originally reach the heart through these newly discovered channels. Further experiments attempted to assess whether hemolymph can also enter the heart through the aorta. Although visualization of flow through the aorta was not possible because of heavy sclerotization, indirect evidence from actin labeling studies showed that the aorta lacks significant musculature and probably collapses during retrograde flow (Fig. 6B). Hence, retrograde hemolymph transport through the aorta is unlikely.

Hemolymph exits the dorsal vessel through excurrent openings located at each end of the vessel. During anterograde flow hemolymph exits through the anterior excurrent opening of the aorta, depositing hemolymph in the head region. This anterior excurrent opening was not directly visualized in this study because of the opacity of the thoracic dorsal cuticle, but flow analysis in the cervix and anterior thorax supports this hypothesis (data not

shown). During retrograde flow hemolymph exits through the caudal excurrent opening of the heart (Fig. 7; supplementary material Movie 7). This excurrent opening is located in the anterior portion of the eighth (last) abdominal segment and is tethered to the tergum by two pairs of bilaterally symmetrical muscle bundles that resemble the anterior halves of alary muscle pairs (Fig. 7A–D). These muscle bundles emerge from two distinct points in the lateral tergum, with the first pair originating near the junction between the seventh and eighth abdominal segments (nearly parallel to the excurrent opening) and the second originating posterior of the caudal end of the heart. Both pairs extend toward the anterior of the insect before binding the heart, and probably function to prevent the heart from being pulled forward during contractions and to facilitate the opening and closing of the excurrent opening. Detailed analysis of numerous preparations suggests that the excurrent opening is composed of two slits formed by the crisscrossing of cardiac musculature to form a laterally oriented figure eight (Fig. 7B,C). The two resultant cavities form the hemolymph exit points, with additional muscle fibers extending toward the posterior of the insect and serve to attach the caudal end of the heart to the tergum. The exact conformation of the excurrent opening varies depending on the contraction state of the heart, but the overall structure more closely resembles the double opening model previously described in Culicidae and Calliphoridae (Iaguzhinskaja, 1954; Jones, 1954; Wasserthal, 1999) than the single opening model described in Drosophilidae (Wasserthal, 2007). Tracking of injected red fluorescent microspheres showed that the posterior excurrent opening allows small volumes of hemolymph to enter the heart when contracting in the anterograde direction while remaining fully open when contracting in the retrograde direction, allowing the entire contents of the vessel to empty into the posterior abdomen at high velocity (Fig. 7E; supplementary material Movie 7).
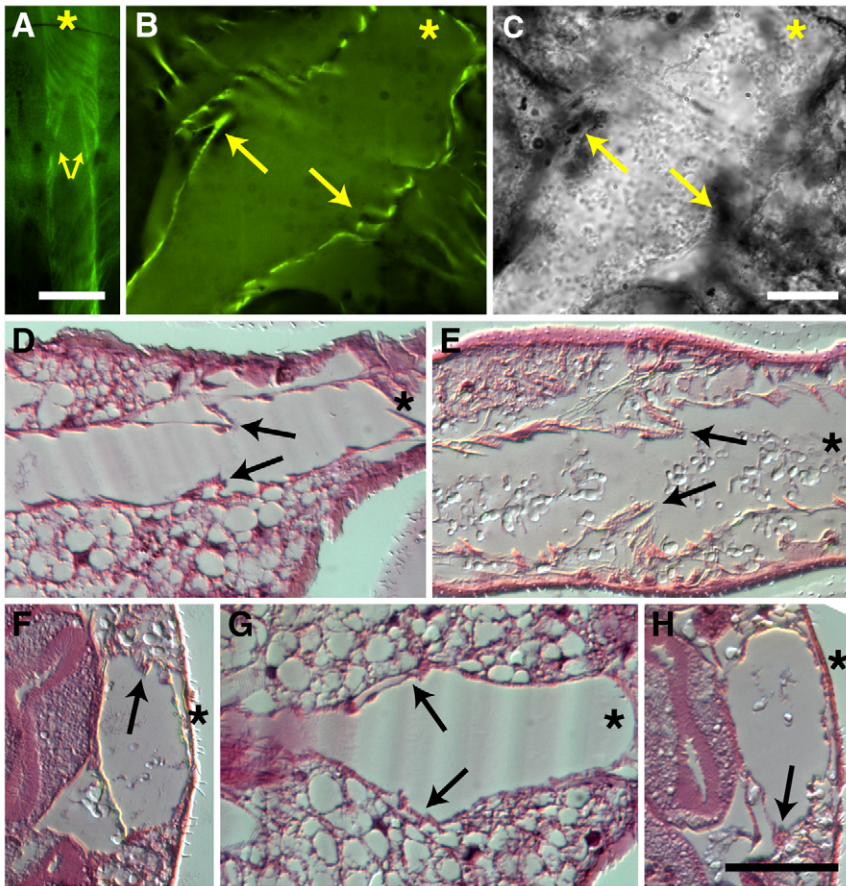
Fig. 5. Incurrent abdominal ostia. Asterisk denotes anterior in A–E and G, and dorsal in F and H. (A) Visualization of labeled muscle through the dorsal cuticle. Ostial lips (arrows) extend from the lateral wall and are angled toward the anterior of the mosquito. (B,C) Fluorescence (B) and bright-field (C) parallel images showing incurrent ostia composed of muscle fibers (B; arrows) and counterstained with India ink (C; arrows). (D–F) Longitudinal (D,E) and cross (F) sections of the heart showing muscular ostia in the open position (arrows). Note that muscle is oriented in a helical twist with respect to the lumen of the vessel. (G–H) Longitudinal (G) and cross (H) sections of ostia in the closed position (arrows). Note that in this static view of peristalsis, heart regions can be seen dilated as wide as 55 µm in diameter as well as completely constricted. Scale bars, (A) 50 µm, (B,C) 20 µm, (D–H) 40 µm.

DISCUSSION

In this study we used state-of-the-art imaging technologies to characterize the structure of the mosquito heart, describe the mechanisms of hemolymph propulsion, and quantify the directionality and speed of hemolymph flow. To our knowledge, this is the first study that visualized insect heart contractions while at the same time measuring hemolymph flow speed and directionality.

The data presented here are in agreement with some of the earlier data analyzing the *Anopheles* heart (Iaguzhinskaja, 1954; Jones, 1954). Both this and earlier studies report the relationship between alary muscles and the heart, describe muscle helically oriented around the lumen of the vessel, and maintain that heart contractions reverse direction. However, our quantitative data show that the resting anopheline heart beats at a slower pace than previously reported and clarifies published discrepancies in the number of ostia present. The
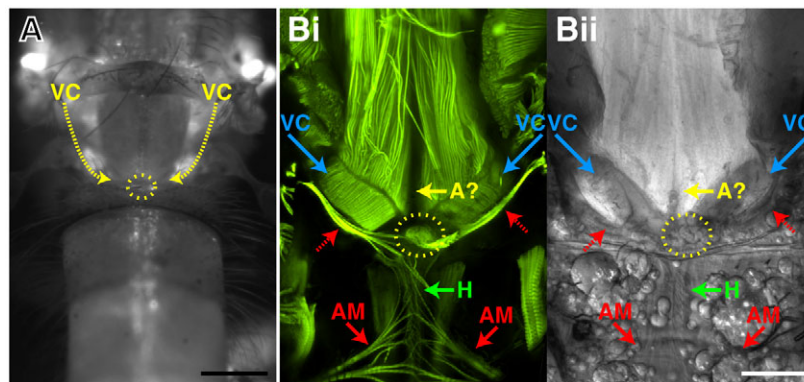

Fig. 6. Venous channels and aorta. Mosquitoes were imaged from the dorsal side and images are oriented with the anterior of the mosquito toward the top. (A) Image of a living mosquito injected with red fluorescent microspheres. Fluorescent flow lines in the lateral posterior thorax (arrows) represent venous channels (VC) that collect hemolymph from the thorax and channel it to thoraco-abdominal ostia (dotted circle) before entering the heart. (B) Fluorescence (Bi) and bright-field (Bii) images of a mosquito dissected along a coronal plane. Labeling of muscle with phalloidin–Alexa Fluor 488 (Bii) showed that the heart (H) is tethered to the aorta and venous channels by musculature that resembles the posterior portion of a pair of alary muscles (red dotted arrows). Hemolymph traveling through the venous channels (VC) enters the heart through a pair of thoraco-abdominal ostia putatively located at the junction between the heart and the aorta (dotted circle). The lack of muscle in the region where the aorta is located (A?) suggests that no significant musculature is associated with that portion of the dorsal vessel. AM, alary muscles. Scale bars, (A) 200 µm, (B) 100 µm.
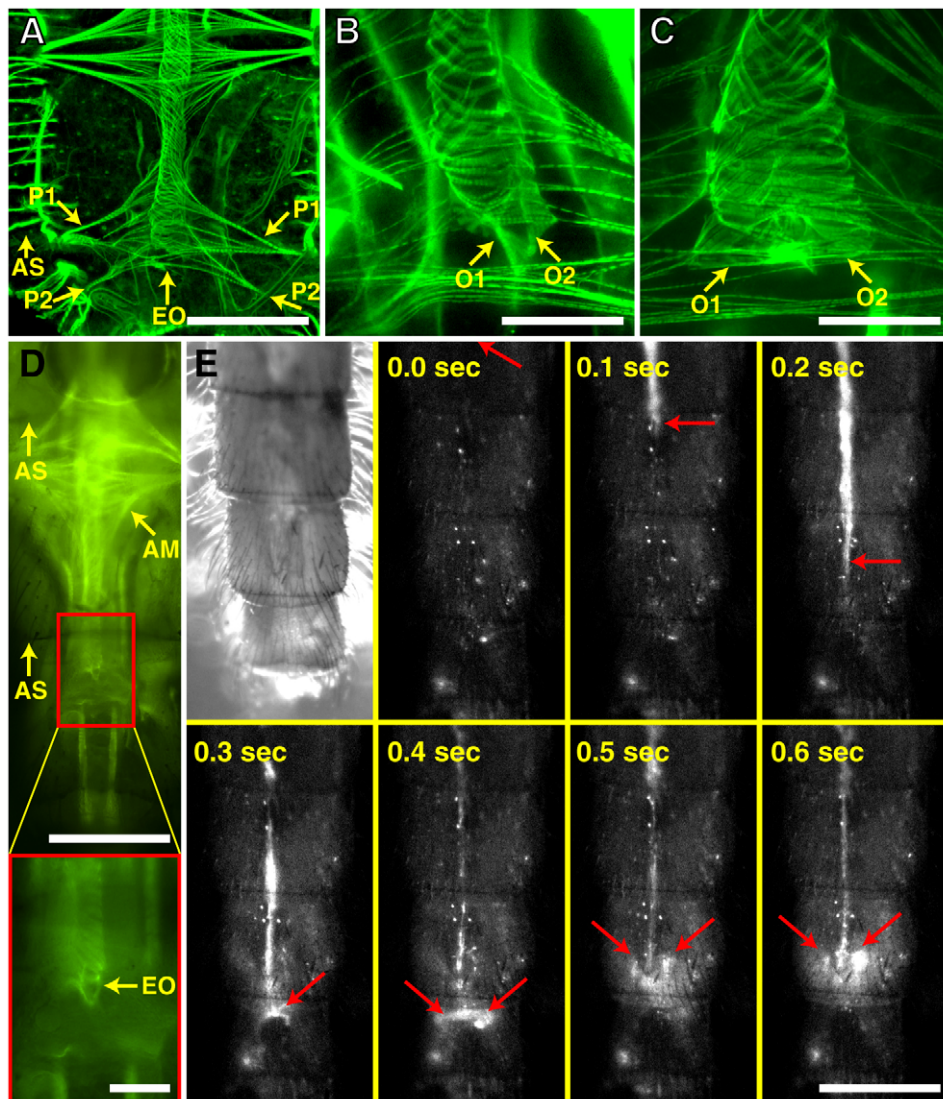
Fig. 7. Posterior excurrent opening (EO) of the heart. All images are oriented with the anterior of the insect toward the top. (A) Fluorescence micrograph of a dissected whole mount showing the two pairs of bilaterally symmetrical muscle bundles (P1 and P2) that tether the posterior end of the heart to the dorsal cuticle. These muscles resemble the anterior portion of alary muscles. AS, abdominal suture. (B,C) Fluorescence micrographs of dissected whole mounts showing two conformations of the excurrent opening. This opening is formed by the crisscrossing of cardiac musculature, forming two hemolymph exit points (O1 and O2). (D) Fluorescence micrograph through the dorsal cuticle showing attachment of the excurrent opening to the tergum. The area inside the square is magnified in the inset. (E) Tracking of a group of red fluorescent microspheres (arrows) in a sequence of consecutive fluorescence images. Microspheres flow in the retrograde direction and exit through the two lateral slits that constitute the excurrent opening. Scale bars, (A,D,D inset) 200 μm; (B,C) 50 μm, (E) 400 μm.

reason for the discrepancies is unclear but is likely due to the limits of the experimental techniques used in those earlier studies. Our use of fluorescently tagged phalloidin allowed for the conclusive visualization of all dorsal musculature, making the number and location of alary muscles absolutely clear. In addition, the tracking of red fluorescent microspheres allowed for the visualization of hemolymph entry into the heart and the absolute determination of the position and number of abdominal ostia. These data are in agreement with our preliminary observations of the heart of *Aedes aegypti* (not shown), and with published data on the number of alary muscles found in that culicine mosquito (Jones, 1977). As for the contraction rate, the elevated number of contractions reported by Jones (Jones, 1954) and Iaguzhinskaja (Iaguzhinskaja, 1954) is probably due to the unnatural mosquito restraint and quantification methods used or the activity state of the mosquitoes. In the study by Jones (Jones, 1954), for example, *An. quadrimaculatus* were restrained by gluing the body to microscope slides and the contraction rate extrapolated using the time required for 10 consecutive heart contractions. It is likely that the firm attachment of mosquitoes using glue prevented the natural contraction of abdominal muscles that may be required for proper heart rhythms (Jones, 1954; Tartes et al., 2002). In addition, the use of short intervals may not have captured natural pauses during

directional switches or brief changes in pulse rates, resulting in an overestimation of contraction velocity. Alternately, the higher heart rates could be attributed to the higher level of activity of the mosquitoes assayed. Our measurements of heart rates of mosquitoes that were more stressfully manipulated by using more forceful restraints or the removal of wings or legs resulted in higher rates (data not shown). With these concerns in mind, our studies used a more natural positioning system that allowed the entire body to rhythmically flex in a natural manner, and measured contractions in each mosquito over a period of 60 consecutive seconds.

Jones (Jones, 1954) also reported that the heart musculature is formed by double bands spaced 5–12 μm apart. Our experimental data do not support the double band model. Contraction of the vessel in conjunction with the tension created by the alary muscles increases and decreases the spacing between individual fibers, meaning that spacing can only be measured relative to location and contraction phase. In addition, Jones (Jones, 1954) reported that severing the alary muscles collapses the abdominal heart chambers, probably impairing hemolymph flow. Although we did not verify this, our observation that the alary muscles physically support the dorsal vessel is in agreement with their hypothesized function in maintaining chamber integrity. Overall, we hypothesize that the

morphological data presented in this report are similar across Culicidae, as their general body plan is conserved (Clements, 1992a).

Heartbeat reversals have been observed in many insect orders, including Lepidoptera, Orthoptera, Homoptera, Ephemeroptera, Neuroptera, Embioptera, Coleoptera, Hymenoptera and Diptera (Gerould, 1933; Jones, 1977; Wasserthal, 1980; Wasserthal, 2007), and are thought to be required for (1) the proper dissemination of molecules throughout the body, (2) thermoregulation, (3) the equilibration of hemolymph pressure, and (4) tracheal ventilation. Studies on lepidopterans and brachyceran dipterans have found that the heart spends the majority of the time contracting in the anterograde direction. However, in some insects retrograde contractions occur at a slower pulse rate than anterograde contractions whereas the opposite occurs in others (Sláma, 2003; Sláma and Farkas, 2005; Sláma and Neven, 2001; Wasserthal, 1999; Wasserthal, 2007). In nematoceran moquitoes we also found that the heart spends the majority of time contracting in the anterograde direction but there was no difference in the pulse rate (Hz) of anterograde *versus* retrograde contractions.

Changes in heart contraction patterns have been described in *Drosophila* using optical and infrared techniques, although the contraction rate and its relation to contraction direction is being debated (Dulcis and Levine, 2005; Wasserthal, 2007). Dulcis and Levine (Dulcis and Levine, 2005) also argued that systole and diastole are synonymous with anterograde and retrograde contractions, respectively, an analysis that has since been challenged (Wasserthal, 2007). Although the differences in contraction mechanics seen in *Drosophila* parallel our morphological observations, our studies show that both anterograde and retrograde contractions contain sequential periods of systole and diastole as hemolymph enters the vessel and is propelled in a bolus-like manner. The biological significance of the changes in contraction mechanics is not clear, but we hypothesize that it may be due to the dynamics of hemolymph entry into the heart. During anterograde contractions hemolymph slowly enters the heart through any of the 12 abdominal ostia or the single pair of thoraco-abdominal ostia. By contrast, all hemolymph pumped in the retrograde direction must enter the heart through the thoraco-abdominal ostia, which receive hemolymph from the venous channels. This distribution may result in differences in hemolymph pressure and volume, necessitating different contraction mechanics.

We also observed that regardless of contraction direction, hemolymph flows through the heart at a velocity greater than $8\,\text{mm}\,\text{s}^{-1}$, indicating that hemolymph can cross the length of the insect in less than one second. The correlative bright field/fluorescence microscopy technique we employed solved the technical limitations faced by researchers who used other direct or indirect techniques to measure either contractions or hemolymph flow, but could not simultaneously measure both. Previous studies using visible light, infrared light, thermography and electrophysiological recordings quantified heart contractions but could not measure absolute flow (Angioy and Pietra, 1995; Dulcis and Levine, 2005; Sláma, 2003; Wasserthal, 1980; Wasserthal, 2007). More recently, a study focusing on the grasshopper *Schistocerca americana* used synchrotron X-ray phase-contrast imaging to measure hemolymph flow speeds by tracking the movement of 10–150 μm diameter buoyant microbubbles (Lee and Socha, 2009), but was unable to visualize the dorsal vessel, ostia or other tissues since this method rendered them transparent. In addition, this latter method employed a restraint system that prevented the natural contraction of abdominal muscles and the ventral diaphragm, probably resulting in altered flow (Tartes et al.,

2002). By contrast, the techniques employed in our study allowed for the simultaneous use of bright-field and low-level fluorescence to visualize both heart contractions and hemolymph flow in an insect restrained in a natural position. This system offers temporal and spatial resolutions that are more sensitive than those for synchrotron X-ray phase-contrast imaging and allow for the tracking of smaller particles, although the latter method probably has a higher capability to track particles deep inside the insect.

Mosquitoes are the most important arthropod vectors of human disease and some of the most studied insects. However, our understanding of their circulatory system lags behind that of other physiological systems. This study presents a comprehensive revision and expansion of our knowledge on the structure and function of the mosquito heart and for the first time quantifies hemolymph flow in an insect while simultaneously observing contracting dorsal vessels. Because of the multifunctional importance of hemolymph flow, we expect that continued studies on the mosquito circulatory system will lead to a better understanding of the interrelation between physiological systems, and the biology of pathogens as they migrate through the hemocoel.

REFERENCES

Angioy, A. M. and Pietra, P. (1995). Mechanism of beat reversal in semi-intact heart preparations of the blowfly *Phormia regina* (Meigen). *J. Comp. Physiol. B: Biochem. Syst. Environ. Physiol.* **165**, 165-170.

Castillo, J. C., Robertson, A. E. and Strand, M. R. (2006). Characterization of hemocytes from the mosquitoes *Anopheles gambiae* and *Aedes aegypti. Insect Biochem. Mol. Biol.* **36**, 891-903.

Chapman, R. F. (1998). Circulatory system, blood, and immune systems. In *The Insects: Structure and Function*, pp. 94-131. Cambridge, UK: Cambridge University Press.

Clements, A. N. (1992a). *The Biology of Mosquitoes*. London: Chapman & Hall.

Clements, A. N. (1992b). The Circulatory System. In *The Biology of Mosquitoes*, vol. 1, pp. 195-205. London: Chapman & Hall.

Dulcis, D. and Levine, R. B. (2005). Glutamatergic innervation of the heart initiates retrograde contractions in adult *Drosophila melanogaster. J. Neurosci.* **25**, 271-280.

Gerould, J. H. (1933). Orders of insects with heart-beat reversal. *Biol. Bull.* **64**, 424-431.

Hertel, W. and Pass, G. (2002). An evolutionary treatment of the morphology and physiology of circulatory organs in insects. *Comp. Biochem. Physiol. Part A Mol. Integr. Physiol.* **133**, 555-575.

Hillyer, J. F. and Christensen, B. M. (2002). Characterization of hemocytes from the yellow fever mosquito, *Aedes aegypti. Histochem. Cell Biol.* **117**, 431-440.

Hillyer, J. F., Barreau, C. and Vernick, K. D. (2007). Efficiency of salivary gland invasion by malaria sporozoites is controlled by rapid sporozoite destruction in the mosquito haemocoel. *Int. J. Parasitol.* **37**, 673-681.

Iaguzhinskaja, L. V. (1954). New results on the physiology and anatomy of the dipteran heart; structure and function of the heart of *Anopheles maculipennis* Mgn. *Biull. Mosk. Obshch. Ispyt. Prir. Otdel. Biol.* **59**, 41-50 (In Russian).

Jones, J. C. (1954). The heart and associated tissues of *Anopheles quadrimaculatus* Say (Diptera: Culicidae). *J. Morphol.* **94**, 71-124.

Jones, J. C. (1977). *The Circulatory System of Insects*. Springfield, IL: Charles C. Thomas.

Klowden, A. J. (2007). Circulatory systems. In *Physiological Systems in Insects*, pp. 357-402. Boston: Academic Press.

Lee, W. K. and Socha, J. J. (2009). Direct visualization of hemolymph flow in the heart of a grasshopper (*Schistocerca americana*). *BMC Physiol.* **9**, 2.

Matuschewski, K. (2006). Getting infectious: formation and maturation of *Plasmodium* sporozoites in the *Anopheles* vector. *Cell Microbiol.* **8**, 1547-1556.

Nation, J. L. (2008). Circulatory system. In *Insect Physiology and Biochemistry*, pp. 339-365. Boca Raton: CRC Press.

Pass, G. (2000). Accessory pulsatile organs: evolutionary innovations in insects. *Annu. Rev. Entomol.* **45**, 495-518.

Pass, G., Gereben-Krenn, B. A., Merl, M. and Plant, J. (2006). Phylogenetic relationships of the orders in Hexapoda: contributions from the circulatory organs for a morphological data matrix. *Arthropod. Syst. Phylogeny* **64**, 165-203.

Salazar, M. I., Richardson, J. H., Sánchez-Vargas, I., Olson, K. E. and Beaty, B. J. (2007). Dengue virus type 2, replication and tropisms in orally infected *Aedes aegypti* mosquitoes. *BMC Microbiol.* **7**, 9.

Sláma, K. (2003). Mechanical aspects of heartbeat reversal in pupae of *Manduca sexta. J. Insect Physiol.* **49**, 645-657.

Sláma, K. and Farkas, R. (2005). Heartbeat patterns during the postembryonic development of *Drosophila melanogaster. J. Insect Physiol.* **51**, 489-503.

Sláma, K. and Neven, L. (2001). Active regulation of respiration and circulation in pupae of the codling moth (*Cydia pomonella*). *J. Insect Physiol.* **47**, 1321-1336.

Tao, Y. and Schulz, R. A. (2007). Heart development in *Drosophila*. *Semin. Cell Dev. Biol.* **18**, 3-15.

Tartes, U., Vanatoa, A. and Kuusik, A. (2002). The insect abdomen – a heartbeat manager in insects? *Comp. Biochem. Physiol.* **133A**, 611-623.

Wasserthal, L. T. (1980). Oscillating haemolymph 'circulation' in the butterfly *Papilio machaon* L. revealed by contact thermography and photocell measurements. *J. Comp. Physiol.* **139**, 145-163.

Wasserthal, L. T. (1999). Functional morphology of the heart and of a new cephalic pulsatile organ in the blowfly *Calliphora vicina* (Diptera: Calliphoridae) and their roles in hemolymph transport and tracheal ventilation. *Int. J. Insect Morphol.* **28**, 111-129.

Wasserthal, L. T. (2007). *Drosophila* flies combine periodic heartbeat reversal with a circulation in the anterior body mediated by a newly discovered anterior pair of ostial valves and 'venous' channels. *J. Exp. Biol.* **210**, 3707-3719.